Computer Modeling in Engineering & Sciences CMES, vol.121, no.2, pp.445-464, 2019

Dynamic Fracture Analysis of Functionally Gradient Materials with Two Cracks By Peridynamic Modeling

Zhanqi Cheng[1], Dongdong Jin[1], Chengfang Yuan[1] and Le Li[1, *]

Abstract: In the research, the dynamic fracture failure problem of functionally graded materials (FGMs) containing two pre-cracks was analyzed using a bond-based Peridynamic (PD) method numerical model. The two convergence of decreasing the area of PD horizon (δ-convergence) and uniform mesh refinement (m-convergence) were studied. The effects of both crack position and distance between two cracks on crack propagation pattern in FGMs plate under tensile loads are studied. Furthermore, the effects of different gradient patterns on the dynamic propagation of cracks in FGMs are also investigated. The simulate results suggest that the cracks positions and the distance between them can significantly influence the dynamic propagation of crack in FGMs. Gradient mode also has a certain effect on crack propagation, but the effect of specific gradient variation patterns on dynamic propagation of crack is finite.

Keywords: Peridynamic, functionally graded materials, crack propagation, dynamic loads.

1 Introduction

Functionally graded materials (FGMs) are a new type of composite materials, which consist of two or more materials. Their composition and structure are continuous gradients. The purpose of FGMs is to eliminate/reduce stress concentration in the material, and improve the bond strength of composites. Generally, FGMs is a kind of multiphase material which can be designed, and the desired material properties can be obtained by controlling the volume ratio of the constituent materials changing along the desired direction. FGM coatings and FGMs can be employed in multitudinous applications involving mechanical studies [Bobaru (2017)].

At present, many components are related to FGMs, therefore, it is of great significance to study and solve the fracture problem of FGMs. On the basis of introducing the concept of FGMs, various aspects of fracture of FGMs under mechanical or thermal loads have been widely studied. Delale et al. [Delale and Erdogan (1983)] studied the crack dynamic propagation of FGM plates with elastic gradients along the crack direction. The results show that the variation of Young's modulus has an effect on the crack propagation in the material, while the Poissons r atio has little effect. It can be seen that the Young's modulus is an important performance parameter for the fracture behavior of FGMs, and the Poisson's ratio does not produce too much image for the stress field. Atkinson and List [Atkinson and List (1978)] conducted a theoretical study on the crack steady-state

[1] School of Civil Engineering, Zhengzhou University, Zhengzhou, 450001, China.

[*] Corresponding Author: Le Li. Email: Lukelee918@163.com.

propagation in materials with variable elastic modulus in space. Kirugulige and Tippur [Kirugulige and Tippur (2006)] used PD theory to simulate the crack dynamic propagation of FGMs materials in mixed-mode. The samples were made of glass-filled epoxy plates with different volume contents, and edge-pre-cracks are set in the gradient direction along the material. In studying the fracture toughness of polymers, Zhuang et al. [Rabczuk, Zhuang, Lahmer et al. (2016); Hamdia, Zhuang, Rabczuk et al. (2017)] proposed a sensitivity analysis toolbox to quantitatively analyze the influence extent of uncertain input parameters on the simulation results, to determine the most important factors affecting the model results, and to obtain the most significant parameters affecting the fracture energy.

Due to the asymmetric material properties of gradient materials, the numerical simulation of it has always been a problem in the computational mechanics, especially its dynamic crack propagation mechanism remains a huge challenge. Kim et al. [Kim and Paulino (2003)] used finite element method to simulate the crack initiation in FGM. They incorporated the mixed mode of T-stress in the material, and studied the crack initiation mechanism in FGM. Liu et al. [Liu, Yao, Ma et al. (2012)] studied the fracture characterizations of mixed-mode crack in FGMs by using digital speckle correlation method (DSCM). Bayesteh et al. [Bayesteh and Mohammadi (2013)] have analyzed the fracture behavior of orthotropic FGMs by using the extended finite element method (XFEM). Petrova et al. [Petrova and Schmauder (2017)] have used the boundary equation methods associated with singular integral equations to study the interaction between edge crack systems and how this interplay affects the formation of crack patterns and the fracture process. Rizov [Rizov (2016)] has analyzed the nonlinear fracture behavior of functionally graded beams by applying the J-integral approach. Zhou et al. [Zhou, Ren, Meng et al. (2017); Zhou, Meng, Li et al. (2016)] proposed a virtual crack closure technique based on non-uniform finite element method, developed a virtual fracture node element for functionally graded materials under dynamic loads, and calculated the energy release rate of functionally graded plates under dynamic loads by Abaqus. Khazal et al. [Khazal, Bayesteh, Mohammadi et al. (2015)] have adopted an extended element free Galerkin method (XEFGM) to simulate the fracture behavior of FGM. The dynamic fracture mechanics of FGMS under thermal shock loading was analyzed by Zheng et al. [Zheng, Yang, Gao et al. (2018)] with a coupled thermoelastic radial integral boundary element method. Rabczuk et al. [Rabczuk and Belytschko (2004); Rabczuk and Belytschko (2007)] presented a meshfree method-EFG-P, in which the modeling of cracks is achieved by discontinuous enrichment, and the method can record the crack propagation path and crack tip expansion speed. Numerical simulation analysis is more suitable for simulating difficult and complex experimental conditions because there are fewer restrictions than experimental and analytical methods. However, the above methods use the classical continuum mechanics model to study the crack problem. Because the calculation equations of the above methods are based on partial differential equations, there are defects in dealing with discontinuity problems in continuous media, especially fracture problems.

Silling et al. [Silling (2000); Silling, Epton, Weckner et al. (2007)] have proposed a new calculation method, Peridynamics (PD), to model and analyze the dynamic fractures at first. The PD is a new non-local successive model in which the equation of motion is represented without spatial derivatives. And for the practicality of PD theory, in the true degree of reaction crack path, Agwai et al. [Agwai, Guven and Madenci (2011)] carried out a number

of experimental studies and finally concluded that PD theory is a high fidelity value in the study of dynamic fracture of objects，and the simulation method can handle numerous cracks and branches. Bobaru et al. [Ha and Bobaru (2011); Ha and Bobaru (2010); Hu, Wang, Bobaru et al. (2013); Hu, Ha and Bobaru (2012); Bobaru, Yang, Alves et al. (2009)] conducted several PD researches of dynamic fracture in composite materials and brittle materials, including impact loading, crack branching and fragmentation. Liu et al. [Liu, Liu and Zhou (2017)] have used the bond-based PD approach to study the fracture of a beam under impact loads with a notch that deviates from the center of the beam. Based on PD theory, Zhang et al. [Zhang, Le, Loghin et al. (2016)] established a fatigue model of two-phase composites and simulated fatigue crack growth. There are multiple crack initiation points in the model, and it is found that the fatigue crack paths interact with each other in a complicated way. Zhou and his co-worker [Gu and Zhou (2017)] have used a fundamental equation of state-based PD theory to simulate the classical fracture process of a single side tensional plate with a circle hole and the propagation and coalescence of cracks in rock under biaxial tensile stress. Zhou et al. [Zhou, Wang and Xu (2016)] simulated a three-point bending test through a non-ordinary state-based PD model, they set a notch in the model that deviates from the center of the beam, and analyzed the crack propagation under quasi-static loading. And Zhou et al. [Zhou and Shou (2017)] developed a new type of bond-based PD method for studying the crack propagation of brittle rock materials. It is well known that rock materials are prone to fracture under stress, or crack propagation and coalescence are more likely to occur in the presence of cracks. Therefore, they studied and analyzed the crack initiation, the law of crack propagation and the coalescence between cracks of brittle rock materials under the compressive loads. Ren et al. [Ren, Zhuang, Rabczuk et al. (2016); Ren, Zhuang and Rabczuk (2017)] further improved the PD formula and presented a dual-horizon PD formula, which allows for simulations with dual-horizon with minimal spurious wave reflection, and demonstrate several advantages of DH-PD on a constant level PD. Yaghoobi et al. [Yaghoobi and Chorzepa (2017)] have proposed a bond-based PD model for simulating dynamic crack propagation in fiber-reinforced concrete. De et al. [De, Zhu and Oterkus (2016)] have researched the influence of fracture toughness, grain size, grain orientation, and grain boundary strength on crack speed, time-to-failure, fracture morphology, and fracture behavior by applying the PD theory. Chowdhury et al. [Chowdhury, Roy, Roy et al. (2016)] have presented a state-based PD formula for simulating the fracture behavior of a shell, and carried out a simulation study of quasi-static crack propagation in the shell. Cheng et al. [Cheng, Zhang, Wang et al. (2015)] proposed a PD model for the dynamic fracture of FGMs, and verified that the PD method can be applied to simulate the brittle fracture behavior of FGMs under dynamic loads. Cheng et al. [Cheng, Liu, Zhao et al. (2018)] studied the dynamic crack propagation and bifurcation of functionally graded plates with pre-cracks under impact loads and dynamic biaxial tensile loads, and analyzed the effects of dynamic load size and material gradient form on crack propagation. In this research, we study the cracks propagation in functionally graded material plates with two cracks under uniform tension with the bond-based PD model, and discuss the effects of crack location, crack spacing and material gradient on the crack growth behavior.

2 PD model for FGMs

2.1 Brief review of PD theory

As shown in Fig. 1, The sample is divided into a number of nodes, where the PD numerical equation at node x and time t is:

$$\rho\ddot{u}(x,t) = \int_H f(u(x,t) - u(\hat{x},t), x - \hat{x})dV_{\hat{x}} + b(x,t) \tag{1}$$

where u is the displacement vector field, ρ is mass density, f is the pairwise force function in the PD bond that connects material points x and $\hat{x}$, and $b(x,t)$ is the body force. The internal region H (see Fig. 1.) called the "horizon region" is defined as

$$H = \{\hat{x} \in R: |x - \hat{x}| < \delta\} \tag{2}$$

Here, δ is "horizon", the size of the nonlocal interaction.

The pair-wise force function derives from the micro-potential function ω:

$$f(\eta,\xi) = \frac{\partial\omega(\eta,\xi)}{\partial\eta} \tag{3}$$

where $\xi = \hat{x} - x$ is the relative position and $\eta = \hat{u} - u$ is the relative displacement between points x and $\hat{x}$. We can obtain the micro-potential function in Eq. (4) when the force magnitude in the material linearly on the relative elongation magnitude.

$$\omega(\eta,\xi) = \frac{c(\xi)s^2\|\xi\|}{2} \tag{4}$$

where $s = \frac{\zeta - \|\xi\|}{\|\xi\|}$ is the relative elongation of a bond, and $\zeta = \|\eta + \xi\|$. The $c(\xi)$ called the micro-modulus function. We can get the following form of pair-wise force function from Eqs. (3), (4).

$$f(\xi,\eta) = \begin{cases} \frac{\xi+\eta}{\|\xi+\eta\|}c(\xi)s & \xi \le \delta \\ 0 & \xi > \delta \end{cases} \tag{5}$$

In this study, the micro-modulus function uses the following equation [Bobaru, Yang, Alves et al. (2009)]:

$$c(\xi) = c_1\left(1 - \frac{\xi}{\delta}\right) = \frac{24E}{\pi\delta^3(1-\upsilon)}\left(1 - \frac{\xi}{\delta}\right) \tag{6}$$

During the deformation of the object, the bond breaks when the length of the PD bond exceeds the critical value (s_0). In the two-dimensional problem, the work required to completely separate an object into two units is called fracture energy G_0, expressed by the following equation:

$$G_0 = 2\int_0^\delta \int_z^\delta \int_0^{\cos^{-1}\left(\frac{z}{\xi}\right)} \left[\frac{c(\xi)s_0^2\xi}{2}\right]\xi d\theta d\xi dz \tag{7}$$

$$s_0 = \sqrt{\frac{5\pi G_0}{9E\delta}} \tag{8}$$

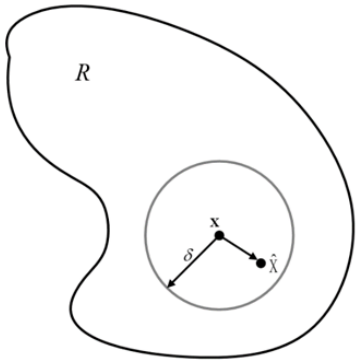

Figure 1: Point x connected with point $\hat{x}$ in the horizon region

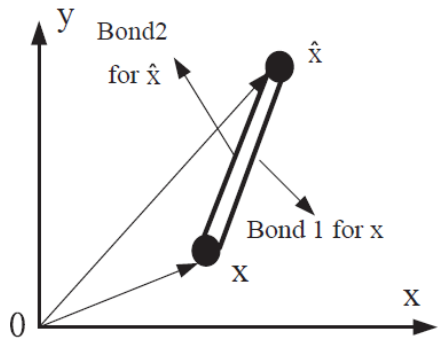

Figure 2: The bonds between points x and $\hat{x}$

2.2 The PD model for FGMs

FGMs are a type of nonhomogeneous composites that is a mixture of two or more materials and both structure and composition are continuously gradients. To simplify the analysis, we assume that the mass density and Youngs modulus of the FGMs have the same form of change and can be depicted as the following functions:

$$E(x,y) = \mathrm{g}(E_0, x, y), \rho(x,y) = \mathrm{g}(\rho_0, x, y) \tag{9}$$

where E_0 and ρ_0 are constants. Delale et al. [Delale and Erdogan (1983)] have proved that the variation in Poisson's ratio ν has a negligible effect on solving the fracture behavior of nonhomogeneous materials, and we can assume that the ν is constant. Hence, for two-dimensional PD numerical models, the value of 1/3 of the Poisson's ratio is used in this paper.

We derived the criteria for fracture energy according to the methods of Kim et al. [Kim and Paulino (2004)]. They are given by:

$$G_0 = \frac{K_{IC}^2(x,y)}{E(x,y)} \tag{10}$$

where E is the Youngs modulus and K_{IC} is the fracture toughness function. Eqs. (6)-(8) are derived from homogeneous materials and its micromodels are constant. However, the FGMs we studied were nonhomogeneous. Therefore, we also use the pair-wise interaction mechanism proposed by Cheng and apply additional hypotheses to derive the general situation of FGMs [Cheng, Liu, Zhao et al. (2018)]. Here, we use two single bonds the same as the original PD bond, as shown in Fig. 2. Both bond 1 and bond 2 are a half of the original interaction and have a half modulus obtained from the node. Accordingly, Eqs. (6) and (8) can be changed to the following equations, separately.

$$c_x(\xi) = c_1\left(1-\frac{\xi}{\delta}\right) = \frac{24E_x}{\pi\delta^3(1-\upsilon)}\left(1-\frac{\xi}{\delta}\right) \tag{11a}$$

$$c_{\hat{x}}(\xi) = c_1\left(1-\frac{\xi}{\delta}\right) = \frac{24E_{\hat{x}}}{\pi\delta^3(1-\upsilon)}\left(1-\frac{\xi}{\delta}\right) \tag{11b}$$

$$s_x = \sqrt{\frac{5\pi G_x}{9E_x\delta}}\ , s_0 = \sqrt{\frac{5\pi G_{\hat{x}}}{9E_{\hat{x}}\delta}} \tag{12}$$

where $E_{\hat{x}}$, $G_{\hat{x}}$, $\rho_{\hat{x}}$, are their effect Young's modulus, fracture energy, and density, respectively. In addition, if one of the two bonds breaks due to reaching the critical elongation, the other bond will also break. Material parameters such as elastic modulus is different in different specimen positions and different horizons, but the relationship between PD parameters (such as s) and material parameters (such as K_{IC}) is independent of the position of the specimen and the horizon.

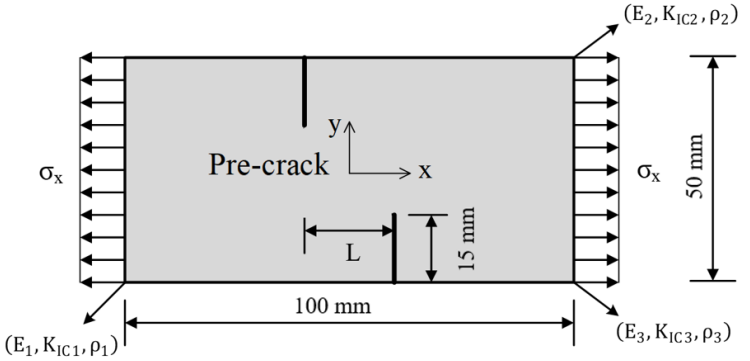

(a)

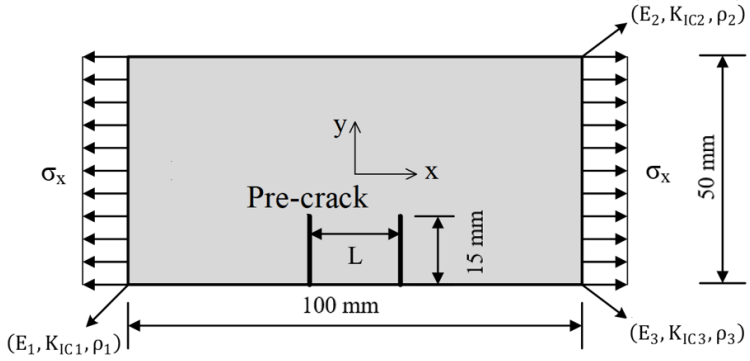

(b)

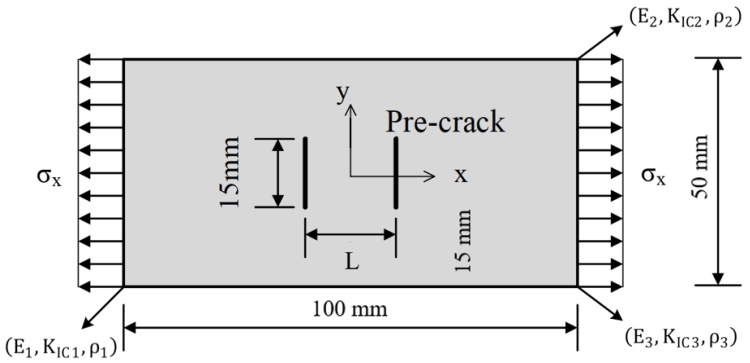

(c)

Figure 3: Sample size and boundary conditions: (a) pre-cracks on different edges, (b) pre-cracks on the same edge, (c) pre-cracks in the middle of the specimen

3 Convergence studies for crack propagation path of FGMs

Cheng et al. [Cheng, Liu, Zhao et al. (2018)] have verified the PD model to get that the model is suitable for analyzing the dynamic fracture behavior of FGMs. In this section, we set the pre-cracks at the edge of the FGMs specimen and study the convergence of the PD in this model by the crack propagation under tensile loads.

3.1 Problem setting

We establish a rectangular FGMs plate measuring 100 mm×50 mm that has two pre-cracks with a length of 15 mm and a spacing of 10 mm (s=10 mm) under dynamic tension loads, as described in Fig. 3(a). The material samples used were made from a mixture of epoxy resin and solid soda-lime balls. The solid soda-lime spheres have different amounts along the diagonal of the sample plate, from 0 to forty percent. The material parameters of the sample plates are shown in Tab. 1 [Rousseau and Tippur (2001)]. A dynamic tension load, $\sigma_x(t)$, is showed in Fig. 4. In this model, we apply uniform tensile loads $\sigma_0 = 10$ MPa on the left and right boundaries of the FGM plate, as shown in Fig. 3. As mentioned above, ν is 1/3.

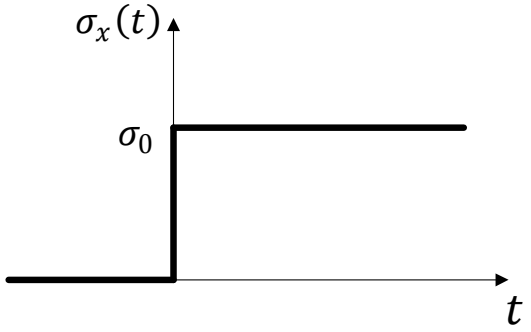

Figure 4: Applied dynamic loads *vs.* time

Table 1: Mechanical properties of FGM samples

E(Pa)	$\rho(kg/m^3)$	$K_{IC}(MPa \cdot m^{1/2})$
$3.8(E_1)$	$948(\rho_1)$	$2.1(K_{IC1})$
$11.1(E_2)$	$1812(\rho_2)$	$3.6(K_{IC2})$

Table 2: Material parameters of FGMs

	$E_3(GPa)$	$\rho_3(kg/m^3)$	$K_{IC3}(MPa \cdot m^{1/2})$
Linear gradient	9.64	1639.20	3.30
Exponential gradient	8.96	1591.80	3.30
Sinusoidal gradient	10.74	1769.71	3.30

3.2 Numerical convergence

In this section, we analyzed the numerical convergence of the FGM plate crack propagation, and tried to control the size of the non-local area to be small enough by simulation. There are two numerical convergence standards in the PD model, δ-convergence and m-convergence. In this section, they are realized through crack paths.

The material properties in the FGM board are expressed by the following functions, the boundary values of which are listed in Tab. 1.

$$E(x,y) = \frac{3.8+11.1}{2} + 58.4x + 29.2y \qquad 0 \le x \le 100mm, 0 \le y \le 50mm \tag{13a}$$

$$\rho(x,y) = \frac{948+1812}{2} + 6912x + 3456y \quad 0 \le x \le 100mm, 0 \le y \le 50mm \tag{13b}$$

$$K_{IC}(x,y) = \frac{2.1+3.6}{2} + 12x + 6y \qquad 0 \le x \le 100mm, 0 \le y \le 50mm \tag{13c}$$

For m-convergence, we conduct the test for the horizon size δ=1.6 mm and used the following values for the m: 3 (Δx=0.67 mm), 4 (Δx=0.5 mm), and 5 (Δx=0.4 mm). The crack propagation of the numerical simulation at 120 s is shown in Fig. 5. We can know that when the ratio of horizon to node spacing is greater than 4 (m>4), the crack path no longer expands further. Additionally, the crack propagation in Figs. 5(b) and 5(c) is substantially identical, indicating that the crack propagation rates are very similar in both cases.

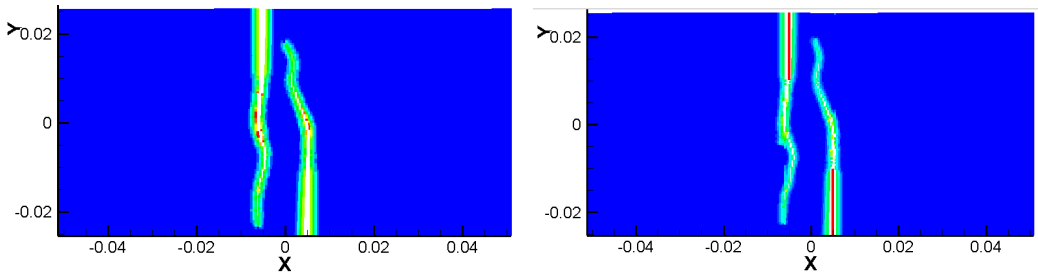

(a) (b)

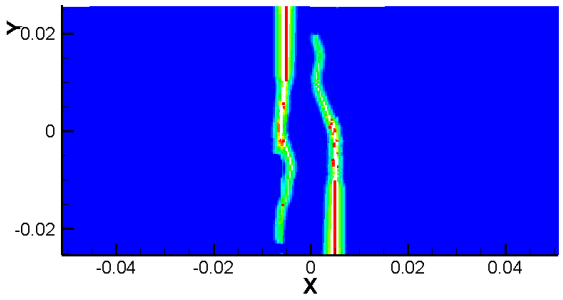

(c)

Figure 5: m-Convergence, the crack path map is at 120 μs: (a) m=3, (b) m=4, and (c) m=5

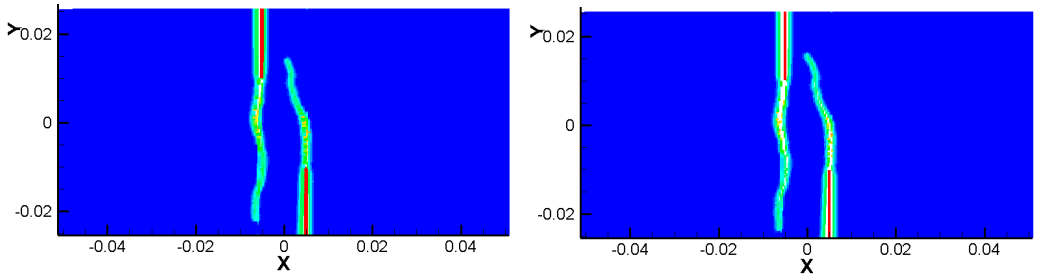

(a) (b)

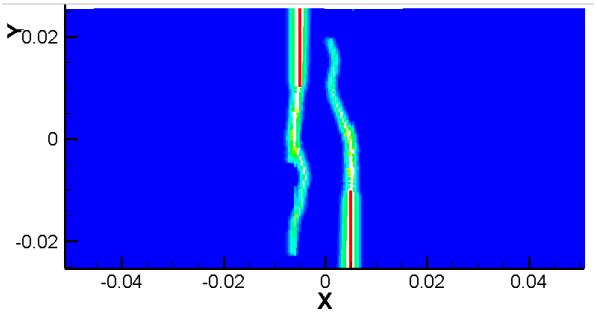

(c)

Figure 6: δ-Convergence, the crack path map is at 120 μs: (a) δ=1.2 mm, (b) δ=1.6 mm, and (c) δ=2 mm

For δ-convergence, we conduct the test for m=4 and applied δ: 1.2 mm, 1.6 mm, and 2 mm for the horizon size. The crack propagation of the numerical simulation at 120 s is shown in Fig. 6. We can know that when the horizon is small enough (δ<1.6), the crack path no longer expands further, and becomes more determined.

Therefore, in the next section, in order to save computational cost and ensure computational accuracy, we keep δ=1.6 mm and m=4.

4 Numerical results of the dynamic fracture of FGMs and discussion

In this section, the effects of three factors will be considered to study the dynamic fracture behavior of FGMs under different conditions.

4.1 Problem setting

We establish a rectangular FGMs plate measuring 100 mm×50 mm that has two pre-cracks with a length of 15 mm. The cracks are arranged symmetrically with respect to y axis and the distance between cracks is L. Symmetrical tensile load are applied to the sheet, as shown in Fig. 3. The material parameters of the sample plates are shown in Tab. 1. A dynamic tension load, $\sigma_x(t)$, is showed in Fig. 4. In this model, we apply uniform tensile loads $\sigma_0 = 10$ MPa on the left and right boundaries of the FGM plate, as shown in Fig. 3. As mentioned above, ν is 1/3.

4.2 Model establishing

In order to study the FGMs fracture behavior under different variations, we studied three variations: linear gradient, exponential gradient and sinusoidal gradient, it is observed that the fracture toughness gradient always displays a linear gradient regardless of the gradient form of the material content. It is assumed that the elastic properties of the FGMs change according to the following equations.

$$E(x,y) = \frac{E_1+E_2}{2} + \gamma_1 x + \gamma_2 y, \rho(x,y) = \frac{\rho_1+\rho_2}{2} + \gamma_3 x + \gamma_4 y \tag{14a}$$

$$K_{IC}(x,y) = \frac{K_{IC1}+K_{IC2}}{2} + \gamma_5 x + \gamma_6 y \tag{14b}$$

$$E(x,y) = \sqrt{E_1 \times E_2} \times e^{(\alpha_1 x+\alpha_2 y)}, \rho(x,y) = \sqrt{\rho_1 \times \rho_2} \times e^{(\alpha_3 x+\alpha_4 y)} \tag{15a}$$

$$K_{IC}(x,y) = \frac{K_{IC1}+K_{IC2}}{2} + \alpha_5 x + \alpha_6 y \tag{15b}$$

$$E(x,y) = E_1 + (E_2 - E_1) \times sin\left(\frac{\pi}{2} \times \left(\mu_1(x+0.05) + \mu_2(y+0.025)\right)\right) \tag{16a}$$

$$\rho(x,y) = \rho_1 + (\rho_2 - \rho_1) \times sin\left(\frac{\pi}{2} \times \left(\mu_3(x+0.05) + \mu_4(y+0.025)\right)\right) \tag{16b}$$

$$K_{IC}(x,y) = \frac{K_{IC1}+K_{IC2}}{2} + \mu_5 x + \mu_6 y \tag{16c}$$

where γ_i(i=1, 2,…6), α_i(i=1, 2,…6), and μ_i(i=1, 2,…6) are calculated from the sample boundary value. E_1, K_{IC1}, ρ_1, and E_2, K_{IC2}, ρ_2, are expressed in Tab. 1. Eqs. (14)-(16) resent three gradients of material properties in the model: linear gradient, exponential gradient, and sinusoidal gradient. The directions of gradient variation can be described by the γ, α, μ in the formulas. The gradient varying simultaneously along x-axial and y-axial will be analyzed below.

Material properties vary diagonally from E_1, ρ_1, K_{IC1} to E_2, ρ_2, K_{IC2}. In order to determine $\gamma_i, \alpha_i, \mu_i$, we have to calculate E_3, ρ_3, K_{IC3} first, the following is the calculation process, the result is shown in Tab. 2.

$$E_3 = 3.8 + (11.1 - 3.8) \times \left(\frac{2}{\sqrt{5}}\right)^2 = 9.64 \tag{17a}$$

$$\rho_3 = 948 + (1812 - 948) \times \left(\frac{2}{\sqrt{5}}\right)^2 = 1639.20 \tag{17b}$$

$$K_{IC3} = 2.1 + (3.6 - 2.1) \times \left(\frac{2}{\sqrt{5}}\right)^2 = 3.30 \tag{17c}$$

$$E_3 = 3.8 \times (11.1/3.8)^{\left(\frac{2}{\sqrt{5}}\right)^2} = 8.96 \tag{18a}$$

$$\rho_3 = 948 \times (1812/948)^{\left(\frac{2}{\sqrt{5}}\right)^2} = 1591.80 \tag{18b}$$

$$K_{IC3} = 2.1 + (3.6 - 2.1) \times \left(\frac{2}{\sqrt{5}}\right)^2 = 3.30 \tag{18c}$$

$$E_3 = 3.8 + (11.1 - 3.8) \times \sin\left(\frac{\pi}{2} \times \left(\frac{2}{\sqrt{5}}\right)^2\right) = 10.74 \tag{19a}$$

$$\rho_3 = 948 + (1812 - 948) \times \sin\left(\frac{\pi}{2} \times \left(\frac{2}{\sqrt{5}}\right)^2\right) = 1769.71 \tag{19b}$$

$$K_{IC3} = 2.1 + (3.6 - 2.1) \times \left(\frac{2}{\sqrt{5}}\right)^2 = 3.30 \tag{19c}$$

Eqs. (17)-(19) calculate respectively the $\mathrm{E_3}, \rho_3, \mathrm{K_{IC3}}$ in the linear function gradient model, exponential function gradient model and sinusoidal function gradient model. Then, we can get $\gamma_i, \alpha_i, \mu_i$.

$$\gamma_1 = \frac{9.64-3.8}{0.1} = 58.4, \quad \gamma_2 = \frac{11.1-9.64}{0.05} = 29.2 \tag{20a}$$

$$\gamma_4 = \frac{1812-1639.2}{0.05} = 3456.0, \quad \gamma_3 = \frac{1639.2-948}{0.1} = 6912.0 \tag{20b}$$

$$\gamma_5 = \frac{3.30-2.1}{0.1} = 12, \quad \gamma_6 = \frac{3.6-3.30}{0.05} = 6 \tag{20c}$$

$$\alpha_1 = \frac{ln\frac{8.96}{3.8}}{0.1} = 8.58, \alpha_2 = \frac{ln\frac{11.1}{8.96}}{0.05} = 4.29, \alpha_3 = \frac{ln\frac{1591.8}{948}}{0.1} = 5.18 \tag{21a}$$

$$\alpha_4 = \frac{ln\frac{1812}{1591.8}}{0.05} = 2.59, \alpha_5 = \frac{3.30-2.1}{0.1} = 12, \alpha_6 = \frac{3.6-3.30}{0.05} = 6 \tag{21b}$$

$$\mu_1 = \frac{arcsin\left(\frac{10.74-3.8}{11.1-3.8}\right)}{\frac{\pi}{2}\times 0.1} = 8, \mu_2 = \frac{(1-0.1\times\lambda_1)}{0.05} = 4 \tag{22a}$$

$$\mu_3 = \frac{arcsin\left(\frac{1769.71-948}{1812-948}\right)}{\frac{\pi}{2}\times 0.1} = 8, \mu_4 = \frac{(1-0.1\times\lambda_1)}{0.05} = 4 \tag{22b}$$

$$\mu_5 = \frac{3.30-2.1}{0.1} = 12, \mu_6 = \frac{3.6-3.30}{0.05} = 6 \tag{22c}$$

From the convergence studies above, we keep δ=1.6 mm and m=4. We use the Verlet algorithm, and the time step takes $\Delta t = 2 \times 10^{-8}\ s$.

4.3 Numerical results and discussion

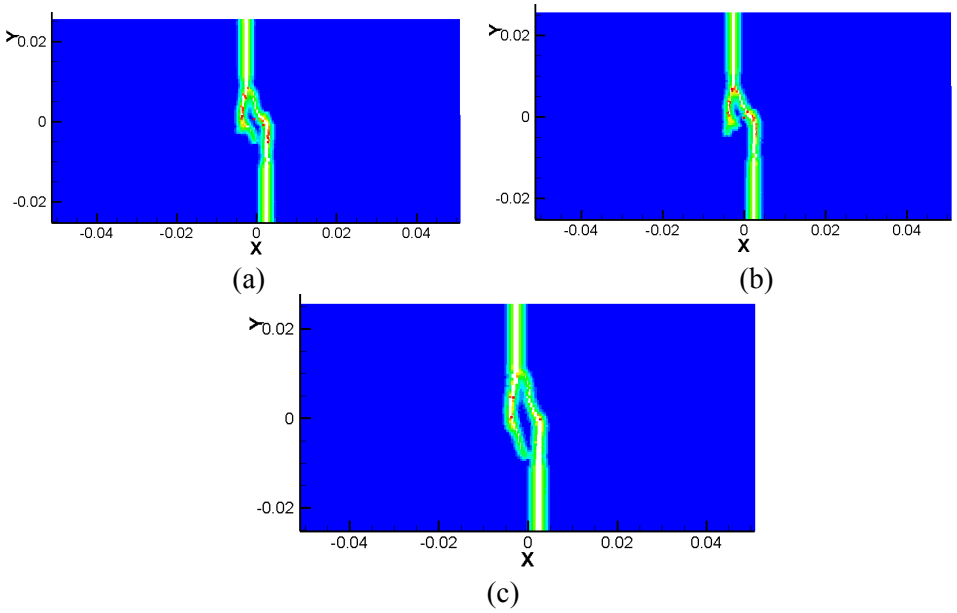

Figure 7: Double cracks on different edges with L=5 mm propagate in FGMs with different graded models: (a) linear graded model. (b) exponential graded model. (c) sinusoidal graded model

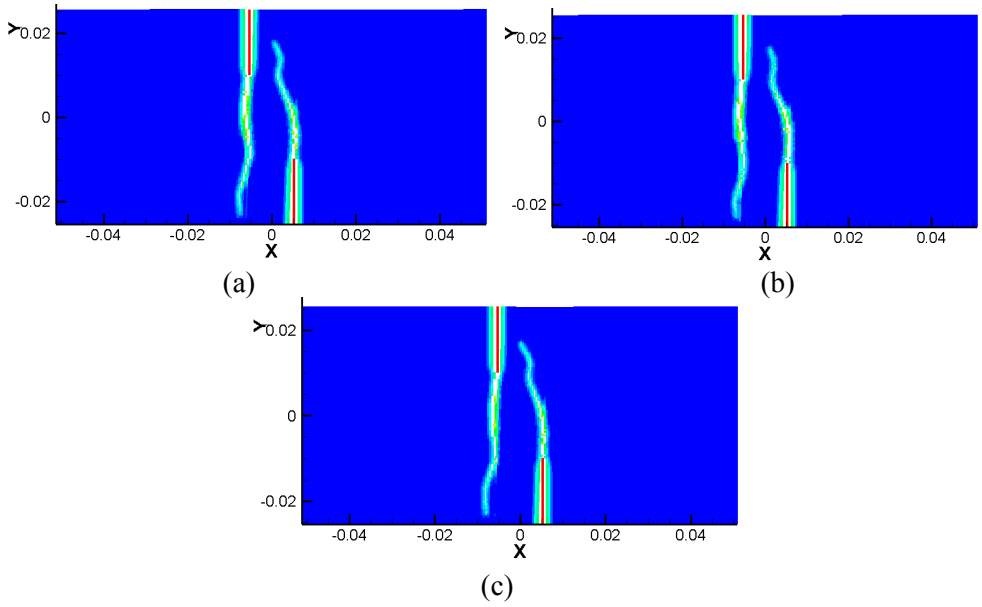

Figure 8: Double cracks on different edges with L=10 mm propagate in FGMs with different graded models: (a) linear graded model. (b) exponential graded model. (c) sinusoidal graded model

In Fig. 9, some snapshots of crack propagation path (both cracks are located in the same side and the distance is L=10 mm) in the FGMs with linear gradient, exponential gradient and sinusoidal gradient, respectively. We can know that the crack growth rate on the left side is always higher, because the gradient material discussed here is bi-directional gradient material, and the stiffness of the material on the left side is smaller. As in shown Fig. 7 and Fig. 8, the specific gradient function of FGMs have no significant effect on the crack growth behavior.

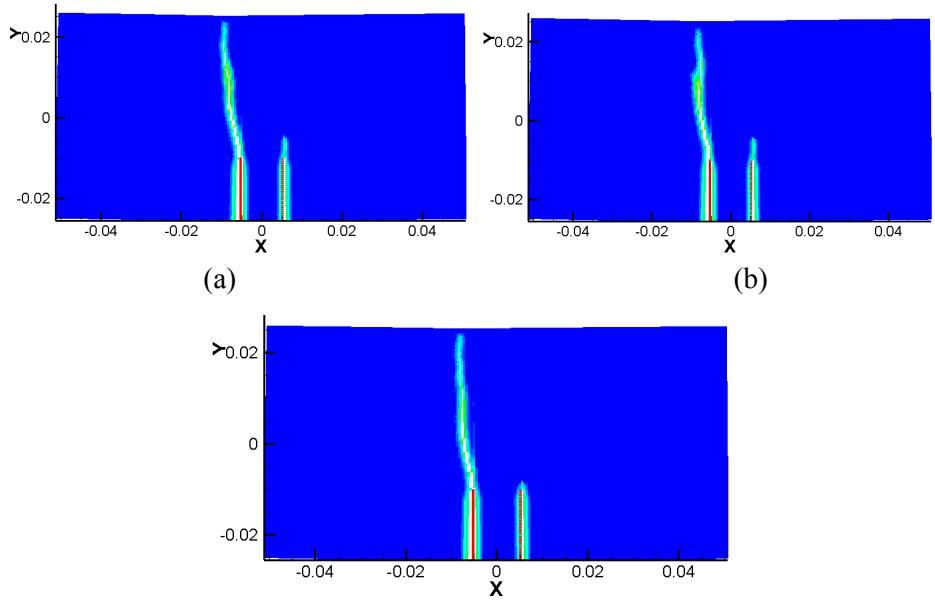

Figure 9: Double cracks on the same edge with L=10 mm propagate in FGMs with different graded models: (a) linear graded model. (b) exponential graded model. (c) sinusoidal graded model

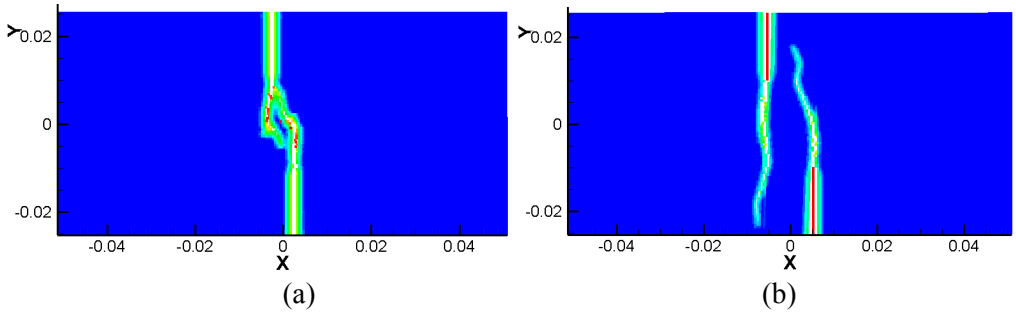

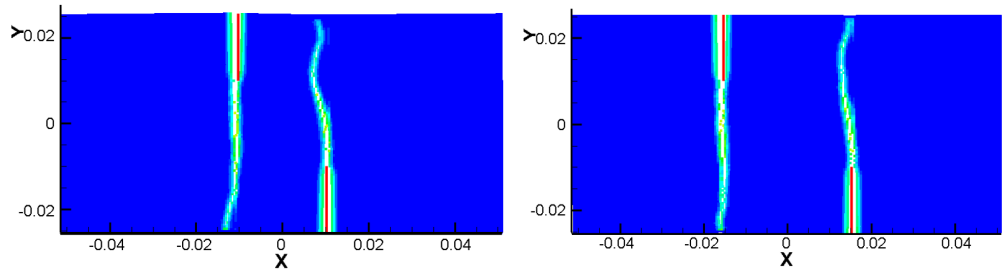

Figure 10: Double cracks on different edges propagate in FGMs with linear graded model: (a) L=5 mm. (b) L=10 mm. (c) L=20 mm. (d) L=30 mm

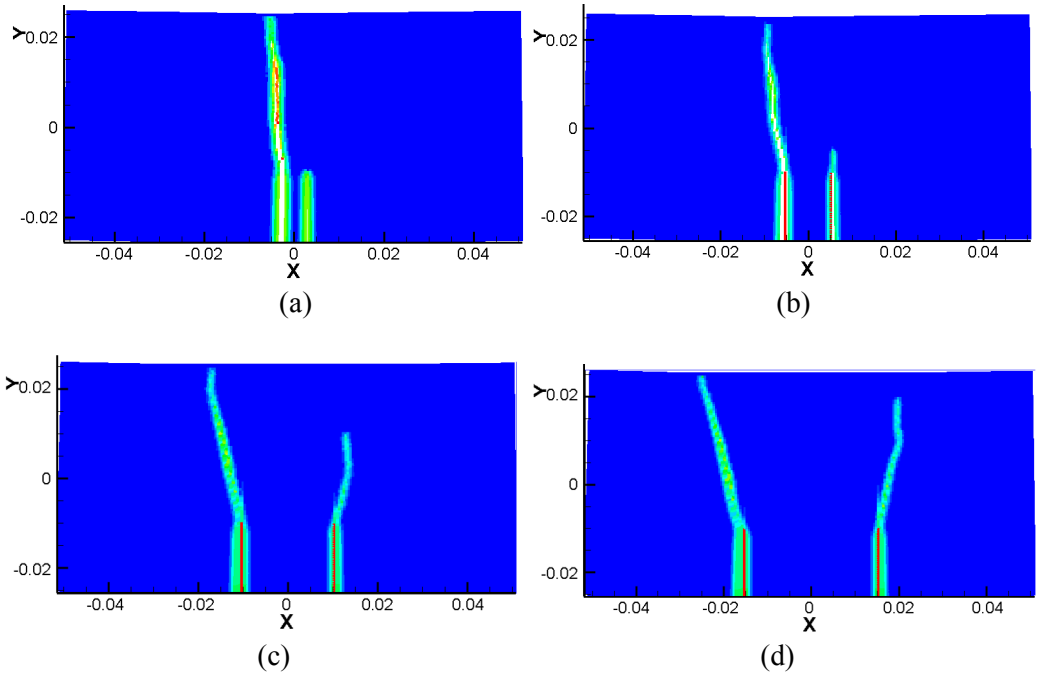

Figure 11: Double cracks on the same edge propagate in FGMs with linear graded model: (a) L=5 mm. (b) L=10 mm. (c) L=20 mm. (d) L=30 mm

Figs. 10-12 show some snapshots of the crack propagation paths of bilateral, single side and intermediate cracks with the crack distance of 5 mm, 10 mm, 20 mm and 30 mm, respectively. It can be found that the propagation paths of cracks at different locations vary greatly. It can also be noticed that when the crack spacing is small (for example L=5 mm or smaller), the propagation behavior of bilateral cracks has a greater effect on each other, while the interaction of cracks at other locations is small, and the interaction decreases with the increase of the crack spacing regardless of where the crack is located.

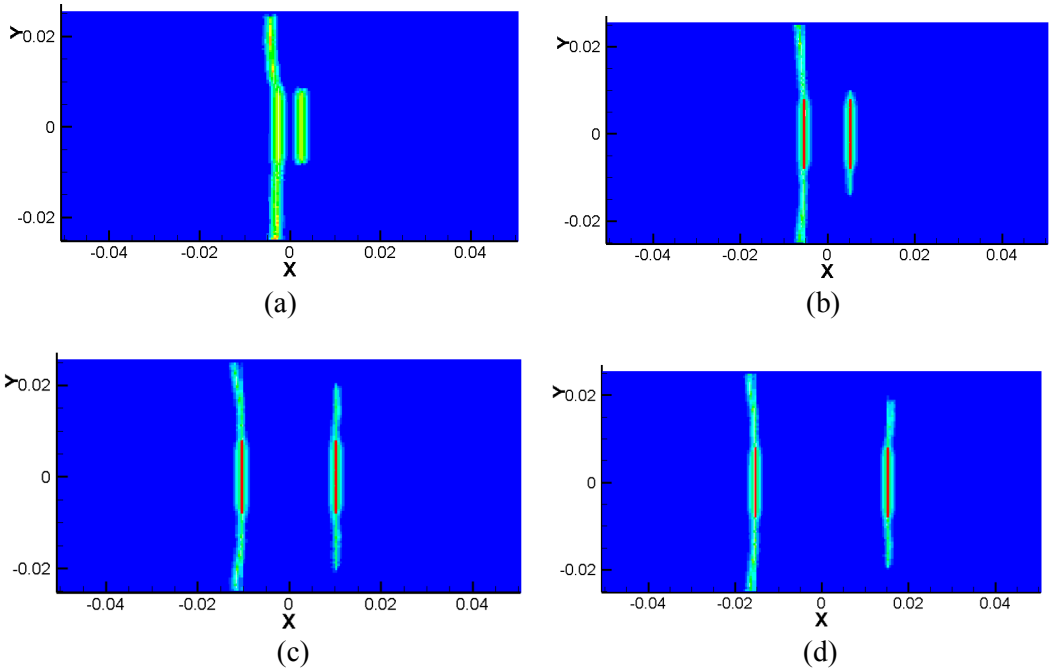

Figure 12: Double middle cracks in the FGMs with linear graded model: (a) L=5 mm. (b) L=10 mm. (c) L=20 mm. (d) L=30 mm

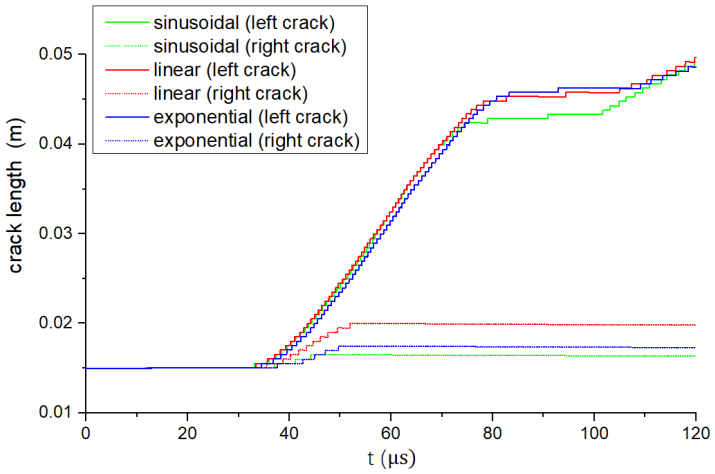

Figure 13: Evolution of crack length in time. The pre-cracks on the same edge with a spacing of 10 mm under different function gradients

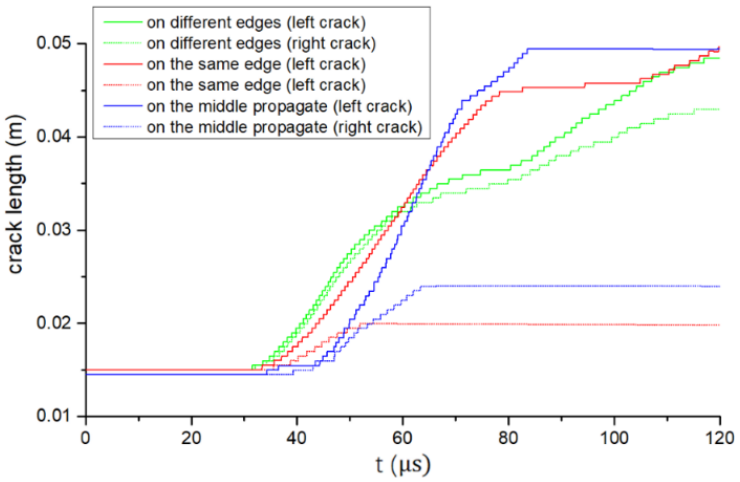

(a)

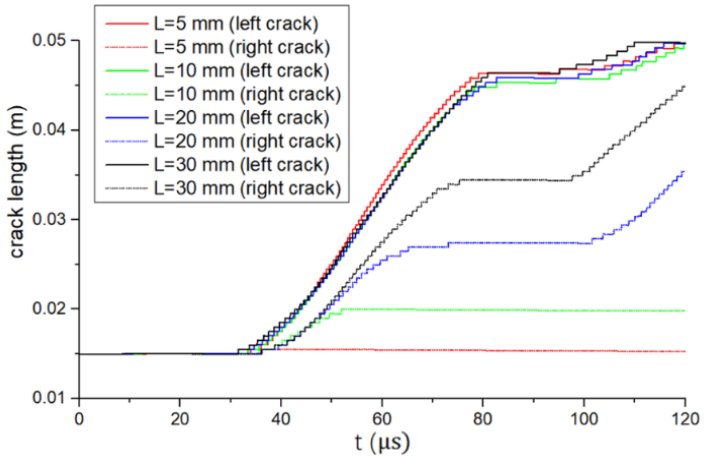

(b)

Figure 14: Evolution of crack length in time. (a): The pre-cracks on different positions with a spacing of 10 mm under a linear function gradient. (b): The pre-cracks on the same edge with different spacings under a linear function gradient

We obtained the crack length from the simulation results, and made a comparison of the crack length under different effect factors, which can reflect the crack growth speed and the crack initiation time. We chose the pre-cracks on the same edge with a spacing of 10 mm to analysis the crack growth under different function gradients, as shown in Fig. 13, we can know that the specific gradient form has an effect on the crack propagation, but not significant. Under the three functional gradients, the crack growth rate is not significantly different. Obviously, the left crack inhibits the right crack growth, due to the left crack tip is more fragile than the right crack tip, and the bond is more easily to break. We chose the linear gradient, and the pre-cracks in different positions with different spacing to analysis the crack propagation, as shown in Fig. 14, it can be seen that the position and spacing of

the two pre-cracks will affect the crack propagation, and the left crack also inhibits the right crack growth. For the case of the pre-crack on different edges, the material properties of the two pre-cracks tip are almost on the same gradient, so the left crack restrains the right crack less. From Fig. 14(b), we can more intuitively find out the effect of the spacing of pre-cracks on crack propagation.

5 Conclusions

The PD method is a method suitable for simulating the dynamic fracture behavior of materials. In this research, the dynamic fracture failure problem of FGMs containing two pre-cracks was analyzed using a bond-based PD method numerical model. Both the effect of crack positions and crack spacings and the influence of gradient patterns of FGMs on crack propagation in FGMs under uniaxial dynamic tensile loads was analyzed. The results suggested that crack positions and spacing of can significantly influence the dynamic propagation of crack in FGMs. Gradient mode also has a certain effect on crack propagation in FGMs, but the effect of specific material gradient variation patterns on crack propagation is finite.

Acknowledgement: This work was supported by the Natural Science Foundation of China (Nos. 11472248, 11872339) and the Natural Science Foundation of Henan Province (No. 182300410221).

References

Agwai, A.; Guven, I.; Madenci, E. (2011): Predicting crack propagation with peridynamics: a comparative study. *International Journal of Fracture*, vol. 171, pp. 65-78.

Atkinson, C.; List, R. D. (1978): Steady state crack propagation into media with spatially varying elastic properties. *International Journal of Engineering Science*, vol. 16, no. 10, pp. 717-730.

Bayesteh, H.; Mohammadi, S. (2013): XFEM fracture analysis of orthotropic functionally graded materials. *Composites Part B-Engineering*, vol. 44, no. 1, pp. 8-25.

Bobaru, F. (2017): Designing optimal volume fractions for functionally graded materials with temperature-dependent material properties. *Journal of Applied Mechanics-Transactions of the ASME*, vol. 74, no. 5, pp. 861-874.

Bobaru, F.; Yang, M.; Alves, L. F.; Silling, S. A.; Askari, E. et al. (2009): Convergence adaptive refinement and scaling in 1D peridynamics. *International Journal for Numerical Methods in Engineering*, vol. 77, pp. 852-877.

Cheng, Z. Q.; Zhang, G. F.; Wang, Y. N.; Bobaru, F. (2015): A peridynamic model for dynamic fracture in functionally graded materials. *Composite Structures*, vol. 133, pp. 529-546.

Cheng, Z. Q.; Liu, Y. K.; Zhao, J.; Feng, H.; Wu, Y. Z. (2018): Numerical simulation of crack propagation and branching in functionally graded materials using peridynamic modeling. *Engineering Fracture Mechanics*, vol. 191, pp. 13-32.

Chowdhury, S. R.; Roy, P.; Roy, D.; Reddy, J. N. (2016): A peridynamic theory for linear elastic shells. *International Journal of Solids and Structures*, vol. 84, pp. 110-132.

De, M.; Zhu, N.; Oterkus, E. (2016): Peridynamic modeling of granular fracture in polycrystalline materials. *Journal of Engineering Materials and Technology-Transactions of ASME*, vol. 138, no. 4.

Delale, F.; Erdogan, F. (1983): The crack problem for a non-homogeneous plane. *Journal of Applied Mechanics-Transactions of the ASME*, vol. 50, no. 3, pp. 609-614.

Gu, X. B.; Zhou, X. P. (2017): Numerical simulation of propagation and coalescence of cracks using peridynamic theory. *Rock and Soil Mechanics*, vol. 38, no. 2, pp. 610-616.

Ha, Y. D.; Bobaru, F. (2011): Characteristics of dynamic brittle fracture captured with peridynamics. *Engineering Fracture Mechanics*, vol. 78, no. 6, pp. 1156-1168.

Ha, Y. D.; Bobaru, F. (2010): Studies of dynamic crack propagation and crack branching with peridynamics. *International Journal of Fracture*, vol. 162, no. 1-2, pp. 229-244.

Hamdia, K. M.; Silani, M.; Zhuang, X. Y.; He, P. F.; Rabczuk, T. (2017): Stochastic analysis of the fracture toughness of polymeric nanoparticle composites using polynomial chaos expansions. *International Journal of Fracture*, vol. 206, no. 2, pp. 215-227.

Hu, W. K.; Wang, Y. N.; Yu, J.; Yen, C. F.; Bobaru, F. (2013): Impact damage on a thin glass plate with a thin polycarbonate backing. *International Journal of Impact Engineering*, vol. 62, pp. 152-165.

Hu, W. K.; Ha, Y. D.; Bobaru, F. (2012): Peridynamic model for dynamic fracture in unidirectional fiber-reinforced composites. *Computer Methods in Applied Mechanics and Engineering*, vol. 217, pp. 247-261.

Khazal, H.; Bayesteh, H.; Mohammadi, S.; Ghorashi, S. S.; Ahmed, A. (2015): An extended element free Galerkin method for fracture analysis of functionally graded materials. *Mechanics of Advanced Materials and Structures*, vol. 23, no. 5, pp. 513-528.

Kirugulige, M. S.; Tippur, H. V. (2006): Mixed-mode dynamic crack growth in functionally graded glass-filled epoxy. *Experimental Mechanics*, vol. 46, no. 2, pp. 269-281.

Kim, J. H.; Paulino, G. H. (2003): T-stress, mixed-mode stress intensity factors, and crack initiation angles in functionally graded materials: a unified approach using the interaction integral method. *Computer Methods in Applied Mechanics and Engineering*, vol. 192, no. 11-12, pp. 1463-1494.

Kim, J. H.; Paulino, G. H. (2004): Simulation of crack propagation in functionally graded materials under mixed-mode and non-proportional loading. *International Journal of Mechanics and Materials in Design*, vol. 1, pp. 63-94.

Liu, N.; Liu, D. S.; Zhou, W. (2017): Peridynamic modelling of impact damage in three-point bending beam with offset notch. *Applied Mathematics and Mechanics-English Edition*, vol. 38, no. 1, pp. 99-100.

Liu, D. L.; Yao, X. F.; Ma, Y. J.; Xu, W. (2012): Study on mixed-mode fracture characterization in functionally graded materials. *Journal of Applied Polymer Science*, vol. 123, no. 4, pp. 2467-2475.

Petrova, V. E.; Schmauder, S. (2017): Modeling of thermomechanical fracture of functionally graded materials with respect to multiple crack interaction. *Physical Mesomechanics*, vol. 20, no. 3, pp. 241-249

Rabczuk, T.; Belytschko, T. (2004): Cracking particles: a simplified meshfree method for arbitrary evolving cracks. *International Journal for Numerical Methods in Engineering*, vol. 61, no. 13, pp. 2316-2343.

Rabczuk, T.; Belytschko, T. (2007): A three-dimensional large deformation meshfree method for arbitrary evolving cracks. *Computer Methods in Applied Mechanics and Engineering*, vol. 196, no. 29-30, pp. 2777-2799.

Ren, H. L.; Zhuang, X. Y.; Cai, Y. C.; Rabczuk, T. (2016): Dual-horizon peridynamics. *International Journal for Numerical Methods in Engineering*, vol. 108, no. 12, pp. 1451-1476.

Ren, H. L.; Zhuang, X. Y.; Rabczuk, T. (2017): Dual-horizon peridynamics: a stable solution to varying horizons. *Computer Methods in Applied Mechanics and Engineering*, vol. 318, pp. 762-782.

Rizov, V. I. (2016): Nonlinear fracture of functionally graded beams under mode II loading conditions. *Strength of Materials*, vol. 48, no. 5, pp. 677-686.

Rousseau, C. E.; Tippur, H. V. (2001): Dynamic fracture of compositionally graded materials with cracks along the elastic gradient: experiment and analysis. *Mechanics of Materials*, vol. 33, pp. 403-421.

Silling, S. A. (2000): Reformulation of elasticity theory discontinuities and long range forces. *Journal of the Mechanics and Physics of Solids*, vol. 48, no. 1, pp. 175-209.

Silling, S. A.; Epton, M.; Weckner, O.; Xu, J. (2007): Peridynamic states and constitutive modeling. *Journal of Elasticity*, vol. 88, no. 2, pp. 151-184.

Vu-Bac, N.; Lahmer, T.; Zhuang, X. Y.; Nguyen-Thoi, T.; Rabczuk, T. (2016): A software framework for probabilistic sensitivity analysis for computationally expensive models. *Advances in Engineering Software*, vol. 100, pp. 19-31.

Yaghoobi, A.; Chorzepa, M. G. (2017): Fracture analysis of fiber reinforced concrete structures in the micropolar peridynamic analysis framework. *Engineering Fracture Mechanics*, vol. 169, pp. 238-250.

Zhang, G. F.; Le, Q.; Loghin, A.; Subramaniyan, A.; Bobaru, F. (2016): Validation of a peridynamic model for fatigue cracking. *Engineering Fracture Mechanics*, vol. 162, pp. 76-94.

Zheng, B. J.; Yang, Y.; Gao, X. W.; Zhang, C. (2018): Dynamic fracture analysis of functionally graded materials under thermal shock loading by using the radial integration boundary element method. *Composite Structures*, vol. 201, pp. 468-476.

Zhou, L. M.; Ren, S. H; Meng, G. W.; Li, R. J. (2017): ABAQUS user subroutine development for energy releasing rate of the functionally graded plate with cracks. *Journal of Northeastern University*, vol. 38, no. 9, pp. 1309-1314.

Zhou, L. M.; Meng, G. W.; Li, X. L.; Li, F. (2016): Analysis of dynamic fracture parameters in functionally graded material plates with cracks by graded finite element method and virtual crack closure technique. *Advances in Materials Science and Engineering*, 8085107.

Zhou, X. P.; Wang, Y. T.; Xu, X. M. (2016): Numerical simulation of initiation, propagation and coalescence of cracks using the non ordinary state-based peridynamics. *International Journal of Fracture*, vol. 201, no. 2, pp. 213-234.

Zhou, X. P.; Shou, Y. D. (2017): Numerical simulation of failure of rock-like material subjected to compressive loads using improved Peridynamic method. *International Journal of Geomechanics*, vol. 17, no. 3.